AMERICAN SOCIETY FOR MICROBIOLOGY | Journal of Virology®

VACCINES AND ANTIVIRAL AGENTS

One-Health: a Safe, Efficient, Dual-Use Vaccine for Humans and Animals against Middle East Respiratory Syndrome Coronavirus and Rabies Virus

Christoph Wirblich,[a] Christopher M. Coleman,[b] Drishya Kurup,[a] Tara S. Abraham,[a] John G. Bernbaum,[c] Peter B. Jahrling,[c,d] Lisa E. Hensley,[c] Reed F. Johnson,[d] Matthew B. Frieman,[b] Matthias J. Schnell[a,e]

Department of Microbiology and Immunology, Sydney Kimmel Medical College at Thomas Jefferson University, Philadelphia, Pennsylvania, USA[a]; Department of Microbiology and Immunology, University of Maryland at Baltimore, Baltimore, Maryland, USA[b]; Integrated Research Facility, National Institute of Allergy and Infectious Diseases, National Institutes of Health, Fort Detrick, Maryland, USA[c]; Emerging Viral Pathogens Section, National Institute of Allergy and Infectious Diseases, National Institutes of Health, Fort Detrick, Maryland, USA[d]; Jefferson Vaccine Center, Thomas Jefferson University, Philadelphia, Pennsylvania, USA[e]

ABSTRACT Middle East respiratory syndrome coronavirus (MERS-CoV) emerged in 2012 and is a highly pathogenic respiratory virus. There are no treatment options against MERS-CoV for humans or animals, and there are no large-scale clinical trials for therapies against MERS-CoV. To address this need, we developed an inactivated rabies virus (RABV) that contains the MERS-CoV spike (S) protein expressed on its surface. Our initial recombinant vaccine, BNSP333-S, expresses a full-length wild-type MERS-CoV S protein; however, it showed significantly reduced viral titers compared to those of the parental RABV strain and only low-level incorporation of full-length MERS-CoV S into RABV particles. Therefore, we developed a RABV-MERS vector that contained the MERS-CoV S1 domain of the MERS-CoV S protein fused to the RABV G protein C terminus (BNSP333-S1). BNSP333-S1 grew to titers similar to those of the parental vaccine vector BNSP333, and the RABV G–MERS-CoV S1 fusion protein was efficiently expressed and incorporated into RABV particles. When we vaccinated mice, chemically inactivated BNSP333-S1 induced high-titer neutralizing antibodies. Next, we challenged both vaccinated mice and control mice with MERS-CoV after adenovirus transduction of the human dipeptidyl peptidase 4 (hDPP4) receptor and then analyzed the ability of mice to control MERS-CoV infection. Our results demonstrated that vaccinated mice were fully protected from the MERS-CoV challenge, as indicated by the significantly lower MERS-CoV titers and MERS-CoV and mRNA levels in challenged mice than those in unvaccinated controls. These data establish that an inactivated RABV-MERS S-based vaccine may be effective for use in animals and humans in areas where MERS-CoV is endemic.

IMPORTANCE Rabies virus-based vectors have been proven to be efficient dual vaccines against rabies and emergent infectious diseases such as Ebola virus. Here we show that inactivated rabies virus particles containing the MERS-CoV S1 protein induce potent immune responses against MERS-CoV and RABV. This novel vaccine is easy to produce and may be useful to protect target animals, such as camels, as well as humans from deadly MERS-CoV and RABV infections. Our results indicate that this vaccine approach can prevent disease, and the RABV-based vaccine platform may be a valuable tool for timely vaccine development against emerging infectious diseases.

KEYWORDS MERS-CoV, coronavirus, immunization, rabies, rhabdovirus

Received 14 October 2016 **Accepted** 30 October 2016

Accepted manuscript posted online 2 November 2016

Citation Wirblich C, Coleman CM, Kurup D, Abraham TS, Bernbaum JG, Jahrling PB, Hensley LE, Johnson RF, Frieman MB, Schnell MJ. 2017. One-Health: a safe, efficient, dual-use vaccine for humans and animals against Middle East respiratory syndrome coronavirus and rabies virus. J Virol 91:e02040-16. https://doi.org/10.1128/JVI.02040-16.

Editor Adolfo García-Sastre, Icahn School of Medicine at Mount Sinai

Address correspondence to Matthias J. Schnell, Matthias.Schnell@jefferson.edu.

Middle East respiratory syndrome coronavirus (MERS-CoV) is a recently emerged highly pathogenic human coronavirus (1). Since its identification in 2012 (2), MERS-CoV has caused over 1,800 infections, with a case fatality rate of ~35% (3). According to epidemiological and sequencing evidence, MERS-CoV is a zoonotic virus that is likely transmitted to humans via the Egyptian tomb bat and one-humped camels. A short piece of the MERS-CoV genome was found in a sample from an Egyptian tomb bat, while several studies have found live MERS-CoV, MERS-CoV RNA, and anti-MERS-CoV antibodies in camels in the Middle East and Africa (4–7). The spread of MERS-CoV from animal reservoirs to humans has been epidemiologically linked, and human-to-human spread has been observed in hospital settings in the Middle East and the Republic of Korea (8–10). The exact mechanism of zoonotic or human-to-human transmission has yet to be established; however, it is presumed to be transmitted by respiratory secretions or small respiratory droplets (11).

The human disease that follows MERS-CoV infection is also poorly understood. The most severely ill MERS patients present with fever, lower respiratory tract symptoms, malaise, and often pneumonia. Chest X rays and computed tomography (CT) scans provide evidence of severe lung inflammation that leads to reduced lung function and death in ~35% of cases (3). Few reports of human autopsy are available, but Ng et al. reported that pneumocytes and epithelial cells are MERS-CoV targets in humans. Evidence of other chronic diseases, including cardiovascular and hepatic diseases, was also noted, further supporting the role of comorbidities in the development of MERS (12).

Research has focused on developing MERS-CoV countermeasures, and several groups have identified drugs, vaccines, antibodies, and other therapeutics that are effective *in vitro* and in small-animal models. Recently, researchers have developed several promising approaches for a MERS-CoV vaccine (13–15; for a review, see references 16–19); however, no vaccines have entered clinical trials or are yet approved for use in humans or other animals.

Most vaccine design has focused on the major immunodominant antigen, the spike (S) protein, located on the surface of the virion, which serves as the ligand for the MERS-CoV receptor dipeptidyl peptidase 4 (DPP4) (also known as CD26) (20). MERS-CoV S is a transmembrane (TM) glycoprotein that is cleaved by the furin protease into the S1 and S2 domains (21). Virus-neutralizing antibodies (VNAs), which are produced in response to infection or vaccination with MERS-CoV S, neutralize virus infection *in vitro* and protect lungs from infection in mouse models of disease (22–25). Vaccine approaches have utilized the MERS-CoV S protein as either a full-length S protein or a recombinant S protein from *Escherichia coli* or insect cells, formulated as nanoparticles (23, 24, 26–29). Other platforms have used plasmid-based expression (25) or expression of MERS-CoV S variants in viral vectors, such as modified vaccinia virus Ankara (MVA) or adenoviruses (22, 30, 31). Each of these different MERS-CoV vaccine approaches comes with individual strengths and weaknesses, such as ease of production, immunogenicity, potential adverse effects, and residual pathogenicity. These factors must be balanced in order to create a vaccine that is ultimately feasible for use in animals and/or humans.

A rhabdovirus-based vaccine offers a combination of features that could prove desirable for an effective MERS-CoV vaccine. Rhabdovirus-vectored vaccine candidates have been developed for several human pathogens (32). More recently, both rabies virus (RABV) and vesicular stomatitis virus (VSV) have been successfully utilized as Ebola virus (EBOV) vaccines, and both approaches are close to clinical trials (RABV) or have already entered phase 2 clinical trials (VSV) (33, 34). Chemically inactivated RABV vaccines are widely used and safe for humans; ~15 million doses of inactivated RABV vaccines are administered to humans every year, with few serious adverse events (35). Both live and chemically inactivated RABV vaccines have been shown to be safe for animals. The live RABV vaccine is widely used in wildlife animals and has successfully eliminated rabies in Western Europe, while inactivated vaccines are used for vaccination of dogs, cats, and ferrets (36). As dual vaccines, RABV-based vectors induce neutralizing antibodies against both RABV and the target pathogen. In a proof-of-

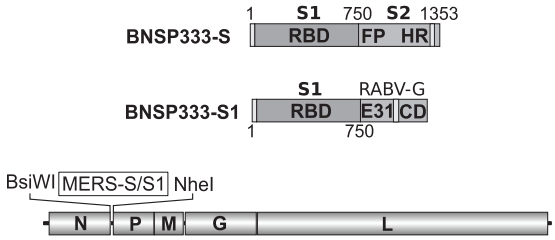

FIG 1 Schematic illustration of the MERS-CoV vaccine constructs used in this study. Spike protein cDNA was inserted between the N and P genes of the SAD-B19-derived RABV vaccine vector BNSP333, which contains a mutation in the glycoprotein gene that eliminates neurotropism of the parent SAD-B19 strain. BNSP333-S contains the wild-type coding sequence of the spike protein of MERS-CoV. The BNSP333-S1-G construct expresses a chimeric protein that contains the entire S1 domain fused to the C-terminal part of the RABV G glycoprotein (amino acids 428 to 524), which encompasses the entire cytoplasmic domain (CD), the TM domain, and 31 amino acids of the ectodomain (E31) of RABV G. Different structural elements of the spike protein are indicated in the full-length construct, including the signal peptide, the receptor-binding domain (RBD), the fusion peptide (FP), heptad repeat (HR) regions 1 and 2, the TM domain, and the CD. Numbers indicate amino acid positions in the spike protein.

concept study, both live-attenuated as well as inactivated RABV-EBOV have been utilized successfully against EBOV (33, 37–40).

To determine if a RABV-based vaccine would be safe and effective against MERS-CoV, we produced a RABV vector that contains the MERS-CoV S1 domains of the MERS-CoV S gene fused to the RABV G protein C terminus. We then chemically inactivated the virus and tested the vaccine in a mouse model of MERS-CoV infection. The mice produced high titers of neutralizing antibodies upon vaccination, and the RABV-MERS S-vaccinated mice were fully protected from MERS-CoV, compared to unvaccinated controls. These data demonstrate the utility of an inactivated RABV-MERS S-based vaccine for blocking MERS-CoV replication *in vivo*, suggesting that RABV-based vaccines have the potential for use in both camels and humans in areas where MERS-CoV is endemic.

RESULTS

Construction of an attenuated RABV expressing the MERS-CoV spike protein. Based on our previous work in constructing a vaccine for EBOV, we chose to introduce the MERS-CoV S protein into the cBNSP333 vector (Fig. 1). MERS-CoV S is a glycoprotein anchored in the membrane of the MERS-CoV virions and therefore a major target for protective antibodies. The BNSP333 vaccine vector utilized here is derived from the attenuated RABV strain SAD-B19 (41). Several modifications were introduced into the parent strain to increase safety and maximize the expression of foreign genes. We have previously shown that foreign genes can be stably introduced into this vector (33, 42–45). Moreover, we showed that the expression of foreign antigens from a position between the RABV N and P genes, as well as codon optimization for human cells of the target gene, results in the highest expression level of the foreign antigen (33). Additionally, replacing arginine with glutamic acid at position 333 (333R→333E) within the RABV glycoprotein (G) further reduces the pathogenicity of the already highly attenuated vector (42). We have successfully used this improved vector to generate candidate vaccines against several emerging zoonotic viral diseases such as EBOV and henipaviruses (33, 45).

Expression of full-length MERS-CoV S inhibits expression of the RABV G protein and reduces viral titers dramatically. We recovered the recombinant BNSP333-S virus and prepared viral stocks of BNSP333-S on Vero cells, which are one of the few cell lines that have been approved by the FDA for the production of human vaccines. When we analyzed the growth kinetics of the recombinant virus in one-step growth curves, we noticed that it reached much lower titers than those of the parent vector BNSP333 (Fig. 2A). In the next step, we analyzed the expression of MERS-CoV S from BNSP333-S. For this approach, Vero E6 cells were infected at a multiplicity of infection (MOI) of 2 with BNSP333-S or BNSP333 as a control (Fig. 2B). Expression of the full-length MERS-CoV S

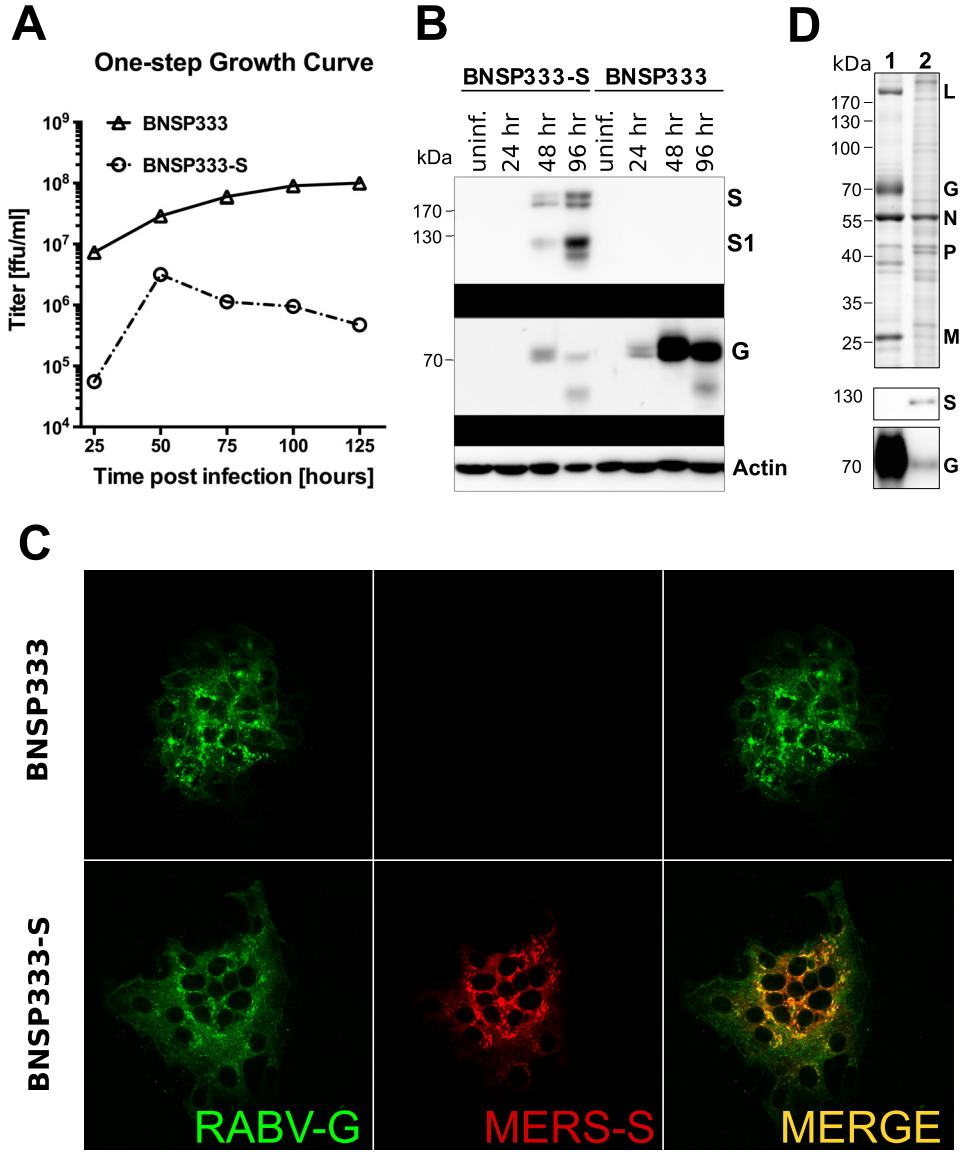

FIG 2 Characterization of BNSP333-S expressing the full-length MERS-CoV spike protein. (A) One-step growth curves on Vero cells demonstrate decreased fitness of the full-length S protein-expressing virus. (B) Western blot analysis of the time course of viral protein expression in Vero cells infected with the parent vector BNSP333 or BNSP333-S demonstrating S protein expression. (C) Immunofluorescence staining of permeabilized Vero cells at 48 h postinfection. Staining of cells infected with BSNP333-S revealed the presence of fused multinucleated cells. (D) SDS-PAGE analysis of purified virions after sucrose gradient purification. Letters indicate the positions of the RABV L, G, N, P, and M proteins. Numbers to the left indicate the sizes of the molecular mass standards. The bottom panel shows Western blot analysis of purified particles probed with anti-S antibody and with monoclonal antibody against RABV G.

protein of ~200 kDa was detected by Western blotting at 48 h postinfection with a monoclonal antibody directed against the S1 subunit. In addition, the antibody revealed a smaller band of ~120 to 130 kDa, which corresponds to the S1 subunit, indicating that the full-length protein is proteolytically cleaved by host cell proteases. We also verified the expression of the RABV glycoprotein. At 48 h postinfection, we observed the typical double band of the RABV glycoprotein at around 70 kDa. However, the expression level of G was much lower in cells infected with BNSP333-S than in cells infected with the parental RABV strain BNSP333 (Fig. 2B). At 96 h postinfection, the amount of the RABV glycoprotein was reduced even more, and only the shorter full-length glycoprotein band was detectable, while an additional truncated band at

around 50 to 60 kDa appeared, indicating proteolytic degradation of the RABV glycoprotein.

To look further into the expression of the two viral glycoproteins, we performed immunofluorescence staining of Vero E6 cells at 48 h postinfection. Both proteins were readily detectable in cells infected with BNSP333-S, whereas only G was detectable in cells infected with the parental virus (Fig. 2C). In terms of viral spread, the two viruses were strikingly different. The parental virus BNSP333 gave rise to medium-sized foci of infected cells, whereas infection with BNSP333-S resulted in mostly large clusters of fused multinucleated cells, likely induced by the MERS-CoV S protein binding to its receptor human DDP4 (hDDP4) (Fig. 2C). Similar observations were made with other heterologous expression systems. When MERS-CoV S proteins were expressed on the surface of hDDP4-expressing cells, they also led to fusion and syncytium formation with neighboring cells expressing the cognate receptor (46).

Because the incorporation of MERS S into RABV particles is a prerequisite for the use of this vaccine in an inactivated form, we purified virus particles from the supernatant of infected Vero cells to analyze their protein content. The particles were concentrated from the clarified cell culture supernatant by ultracentrifugation on sucrose cushions and resolved on sodium dodecyl sulfate (SDS)-polyacrylamide gels. After staining with Sypro ruby, several protein bands were detected for BNSP333, and these bands corresponded in size to the RABV N, P, M, G, and L proteins (Fig. 2D). However, the virions collected from the supernatants of cells infected with BNSP333-S seemed to contain no RABV G protein or at least a greatly reduced amount. Additional bands of the expected size for the MERS-CoV S protein (180 kDa) and the S1 subunit (110 to 120 kDa) were detectable in the BSNP333-S virion preparation. However, these bands were rather faint. To verify the presence of the MERS-CoV spike protein as well as to confirm the reduced level of RABV G, we performed a Western blot (WB) analysis. Using a monoclonal antibody specific for MERS-CoV S1, we detected the 120-kDa S1 subunit in BNSP333-S virions but no full-length S protein. As expected, no S-reactive bands were detected in the control virus BNSP333. Using a mixture of monoclonal antibodies directed against RABV G, we confirmed that the incorporation of RABV G is greatly reduced in BNSP333-S virions (Fig. 2D, bottom). Collectively, these data showed that the expression of the full-length S protein interferes with viral protein expression, in particular the expression of RABV G, resulting in reduced particle assembly and viral titers. The BNSP333-S construct was therefore considered unsuitable for further development of the MERS-CoV vaccine.

Expression of S1 fused to the C-terminal part of RABV G results in strong incorporation of the RABV G–MERS-CoV S1 fusion protein. Previous studies have shown that the fusion domain of MERS-CoV S is located within the S2 subunit of MERS-CoV S, whereas the S1 subunit of MERS-CoV S contains the receptor-binding domain (RBD). Moreover, research by others indicates that antibodies directed against the RBD can protect against disease (23, 24), and therefore, the expression of S1 might be sufficient to induce protective immune responses against MERS-CoV. Hence, we constructed a new vaccine vector (BNSP333-S1) expressing the N-terminal 750 amino acids (aa) of MERS S fused to a truncated RABV glycoprotein, which comprises 31 aa of the ectodomain (ED), the complete cytoplasmic domain (CD), and the transmembrane domain of RABV G to allow chimeric glycoprotein incorporation into RABV virions. The chimeric MERS-CoV S1–RABV G protein utilizes the original MERS-CoV endoplasmic reticulum (ER) translocation sequence and was generated by PCR of codon-optimized cDNA fragments (Fig. 1).

Infectious virus was recovered as described above. One-step growth curves showed that the new virus expressing only S1 grew to titers of roughly 10^8 focus-forming units (FFU)/ml, which were similar to those of the control virus BNSP333 on Vero cells (Fig. 3A). To verify the expression of the chimeric S1-G glycoprotein, we infected Vero cells at an MOI of 2 and collected the cell lysate over a period of 4 days. Western blot analysis of the cell lysate indicated the presence of a strong double band of approximately 120 to 150 kDa in cells infected with BNSP333-S1, which reacted strongly with antibodies

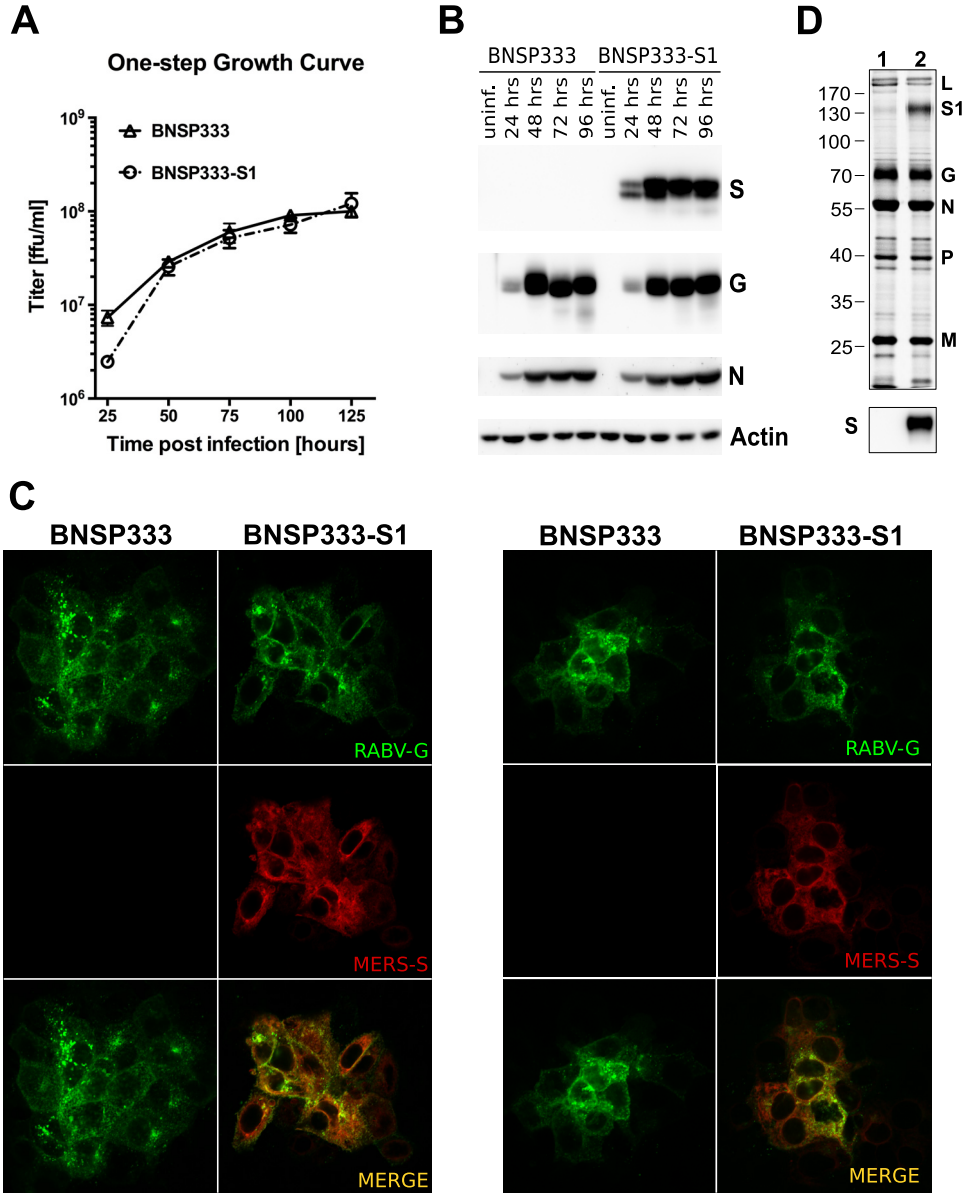

FIG 3 Characterization of BNSP333-S1 expressing a chimeric S1-G fusion protein. (A) One-step growth curves on Vero cells. (B) Time course of protein expression in infected Vero cells. (C) Immunofluorescence staining of permeabilized Vero cells at 48 h postinfection labeled for either the RABV G protein or the MERS-CoV S protein. (D) SDS-PAGE analysis of purified virions after sucrose gradient purification. Letters indicate the positions of the RABV L, G, N, P, and M proteins. Numbers to the left indicate the sizes of the molecular mass standards. The bottom panel shows Western blotting of purified particles probed with anti-S antibody.

specific for the S1 subunit of MERS-CoV S and was absent in cells infected with the control virus BNSP333, confirming the expression of the S1-G fusion protein (Fig. 3B). In contrast to the virus expressing full-length S, no difference in the expression of the RABV glycoprotein was detectable between cells infected with BNSP333-S1 and cells infected with the parent virus BNSP333. Finally, immunofluorescence analysis showed that Vero E6 cells infected with BNSP333-S1 coexpress RABV G and the S1-G chimera and do not form the multinucleated syncytia that we observed when cells were infected with BNSP333-S (Fig. 3C).

To analyze the incorporation of the chimeric glycoprotein into RABV particles, Vero cells were infected with BNSP333 or BNSP333-S1, and virus particles were purified. SDS-PAGE analysis of the purified virions revealed a strong band of ~150 kDa in the supernatant of Vero cells infected with BNSP333-S1 (Fig. 3D), which reacted strongly

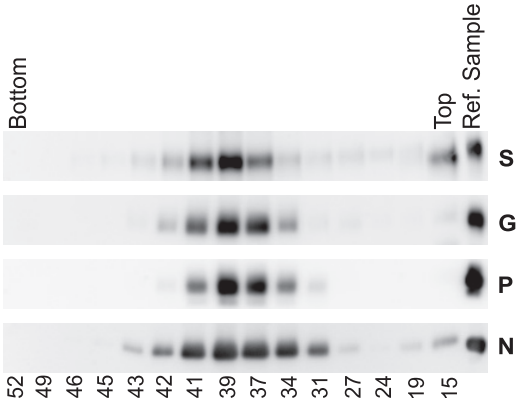

FIG 4 The S1-G chimera is incorporated into virions. Particles collected from the supernatant of infected Vero E6 cells were centrifuged on a 15 to 65% linear sucrose gradient. Viral proteins were detected in the collected fractions by Western blotting with the indicated antibodies. MERS-CoV S peaked in fraction 17, as did the RABV G, N, and P proteins. The rightmost lane shows particles pelleted from the supernatant of infected Vero cells. Numbers at the bottom show the sucrose concentrations in the collected fractions.

with antibodies specific for the S1 subunit of MERS-CoV S and was absent in the control virus, indicating the efficient incorporation of the S1-G fusion protein into BNSP333-S1 particles (Fig. 3D, bottom). Both the control virus BNSP333 and the BNSP333-S1 virus preparations contained similar amounts of RABV G. To confirm that the S1-G protein is indeed incorporated into RABV particles and does not merely copurify with RABV virions containing only G, we sedimented virions on a linear sucrose density gradient. The gradient was fractionated and analyzed for protein content by Western blotting. As shown in Fig. 4, we observed a small amount of S-reactive material at the top of the gradient. However, most of the S1 signal peaked in fraction 17 at the same density as the RABV G, N, and P proteins, which strongly suggests that the S1-G chimeric protein is indeed incorporated into RABV virions. To provide further evidence for this conclusion, we performed immunogold labeling of Vero E6 cells infected with BNSP333-S1 (Fig. 5). Virions labeled with antibodies specific for the S1 (Fig. 5, large dots) and RABV G (small dots) proteins were observed budding from infected cells, clearly showing that both proteins are incorporated into RABV particles. Collectively, these data showed that the S1-G protein that lacks the S2 subunit no longer interferes with RABV G expression and particle assembly and most importantly is efficiently expressed and incorporated into virions, thus making BNSP333-S1 a suitable vaccine candidate.

BNSP333-S1 is immunogenic in mice and protects against challenge with MERS-CoV. To analyze the immunogenicity of BNSP333-S1, we immunized 4 groups of BALB/c mice (5 mice per group) with 10 μg of BNSP333-GP (group 1), 10 μg of BNSP333-S1 (groups 2 and 3), or phosphate-buffered saline (PBS) (group 4) at days 0,

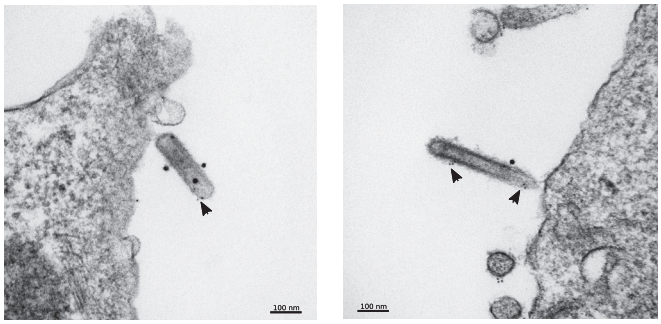

FIG 5 Immunoelectron microscopy of Vero E6 cells infected with BNSP333-S1. Filled arrowheads pointing to small gold particles indicate labeling with monoclonal antibody specific for RABV G. Large gold particles indicate staining with anti-S polyclonal rabbit serum.

7, and 21 postinoculation. We monitored the immune response against RABV G and MERS-CoV S by antigen-specific enzyme-linked immunosorbent assays (ELISAs). The antigen-specific IgG responses increased over time and after each immunization; they reached high antibody levels against both RABV G and MERS-CoV S after the third inoculations. MERS-CoV S-specific immune responses were detected only in groups 2 and 3, but RABV G-specific IgG was detected in groups 1 to 3 (Fig. 6). None of the animals of group 4, which were mock immunized, demonstrated immune responses against the RABV G or MERS-COV S protein, confirming the specificity of the ELISAs. Whereas RABV G-specific ELISA titers are known to predict protection against RABV challenge (47–49), the protective abilities of the MERS-CoV S-directed antibodies are unknown. We therefore performed VNA assays against MERS-CoV using sera collected on day 35 postimmunization from mice of all four groups (Fig. 7). We detected low levels of MERS-CoV-neutralizing antibodies in the sera of mice from group 1 (BNSP333-GP) or mock (PBS)-immunized mice (group 4), but the sera of mice immunized with BNSP333-S1 (groups 2 and 3) neutralized MERS-CoV at serum dilutions of between 1:1,280 and 1:5,120. This demonstrates that high levels of anti-MERS-CoV-neutralizing antibody were produced in the BNSP333-S1-vaccinated mice.

Efficacy testing of the RABV-MERS vaccine was performed by using the adenovirus-hDPP4-transduced mouse model (50). All four groups of mice were transduced, and after 5 days, mice in groups 1, 2, and 4 were challenged intranasally (i.n.) with MERS-CoV at 1×10^5 PFU/mouse (strain Jordan-n3/2012). Four days after challenge, the mice were euthanized, and their lungs were dissected, homogenized, and assayed for viral loads by reverse transcription-quantitative PCR (qRT-PCR) and a viral plaque assay. For BNSP333-S1-immunized mice, levels of both genomic RNA and mRNA were reduced to background levels similar to those found in mice not transduced by adenovirus 5 (Ad5) expressing hDPP4 (Table 1). Moreover, immunization with BNSP333-S1 reduced the viral load in the lungs to a level below the limit of detection of the assay (2.5×10^2 PFU/g of lung) (Table 2).

DISCUSSION

In this study, we describe a novel RABV-based vaccine expressing the MERS-CoV S1 protein as a potential vaccine against MERS-CoV. Similar to our previous vaccine approaches, we expressed the target antigen for the vaccine (MERS-CoV S) from the highly attenuated RABV vector BNSP333 (42). For our initial BNSP333-S candidate, we observed that MERS-CoV S expression dramatically reduced the expression of RABV G and incorporation into virions. Furthermore, RABV virions contained only a small amount of MERS-CoV S. Similar findings were observed with a VSV vector, where again the expression of MERS-CoV S from the genome led to low levels of VSV G in the virions (data not shown).

Therefore, based on our previous work in which we successfully expressed different viral glycoproteins from RABV-based vectors and noticed only modest effects on viral replication kinetics and final titers (33, 38, 44, 45, 51–53), we hypothesized that the retention of the MERS-CoV S protein in the ER may have a detrimental effect on the expression and processing of RABV G in the ER and/or Golgi apparatus. We excluded another hypothesis, that the heavy glycosylation of MERS-CoV S was responsible, based on the fact that both the HIV-1 glycoprotein gp160 and Ebola virus GP are heavily glycosylated but also well expressed from RABV, and they are incorporated into virions without inhibiting RABV G incorporation (38, 44, 54).

We took an alternative approach to the expression of the full-length MERS-CoV S protein by focusing on the expression of MERS-CoV S1, which contains the RBD; the RBD has been shown to be sufficient to induce VNA against MERS-CoV (23, 24, 29). Because the MERS-CoV S1 protein is secreted due to the lack of a membrane anchor (55–57), we fused S1 to the C-terminal part of RABV G to direct MERS-CoV S1 into budding RABV virions. The use of the part of the RABV G extracellular domain containing the potential trimerization domain, in addition to the RABV G TM domain and CD, proved useful for the highly efficient incorporation of foreign glycoproteins

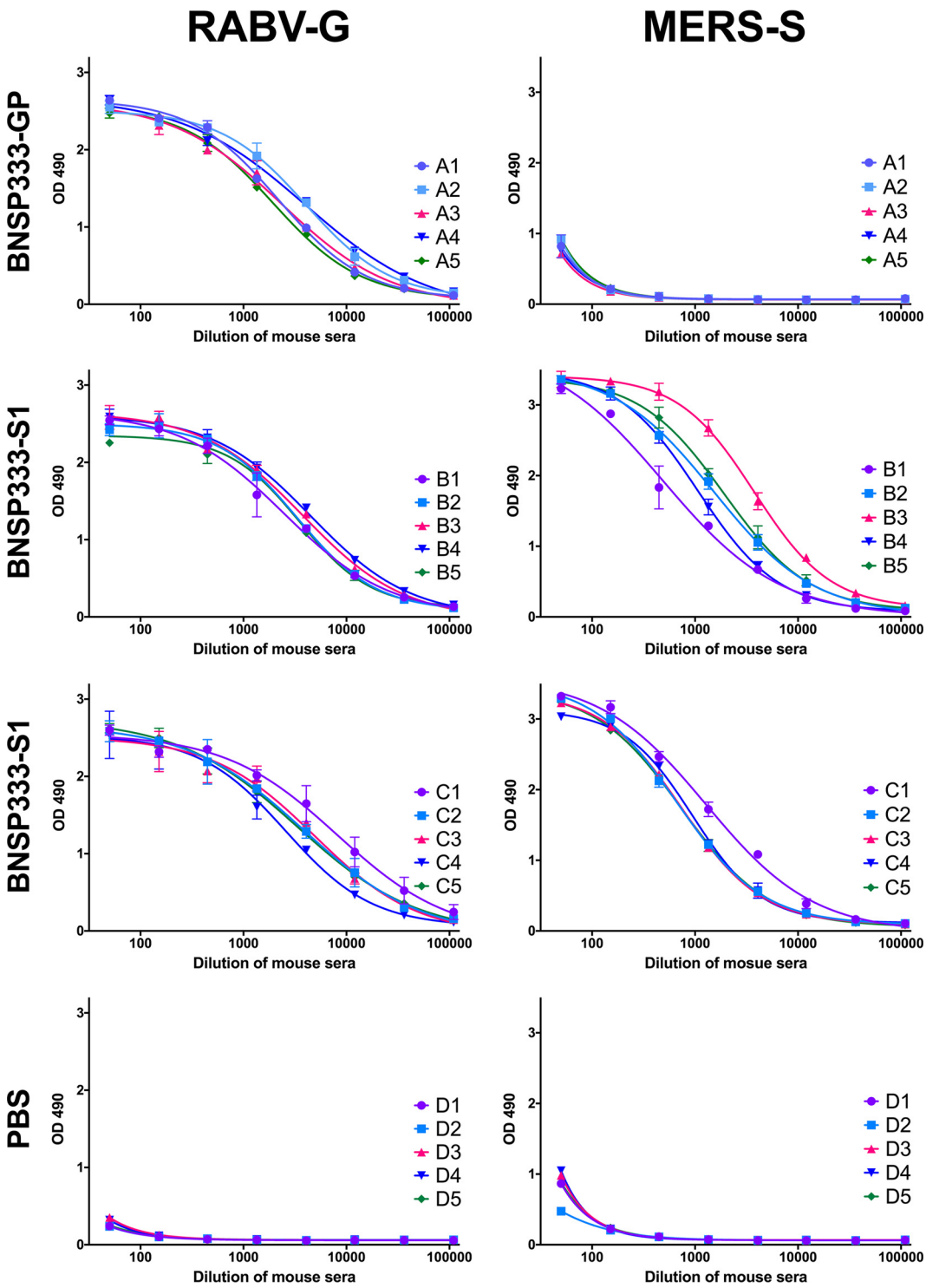

FIG 6 Analysis of the immune response to BNSP333-S1 in mice. BALB/c mice were immunized three times (days 0, 7, and 21) with 10 μg chemically inactivated particles of BNSP333-S1 (groups B and C) ($n = 10$) or BNSP333-GP (BNSP333 expressing Zaire ebolavirus GP) (group A) ($n = 5$) or mock immunized with PBS (group D, $n = 5$). Serum was collected from each mouse at day 35 for analysis by a MERS-CoV S-specific ELISA. All mice immunized with BNSP333-S1 developed a strong humoral immune response to the S1 subunit and RABV G. No response above background levels was detected in unvaccinated control mice (PBS group). OD, optical density.

into rhabdoviruses (43, 51). In contrast to MERS-CoV S, the MERS-CoV S1–RABV G fusion protein was efficiently incorporated into the RABV virions.

A good animal model is essential for vaccine research. MERS-CoV can cause transient lower respiratory tract infection in rhesus macaques, but the disease is mild compared

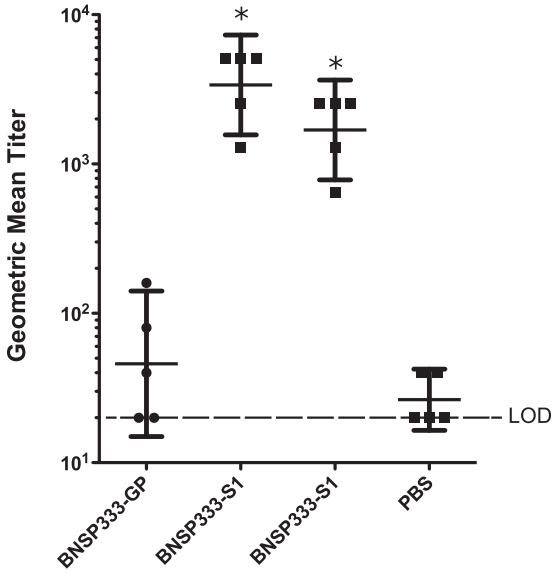

FIG 7 Sera from BNSP333-S1-vaccinated mice neutralize MERS-CoV. Sera collected on day 35 were assayed in neutralization assays against MERS-CoV on Vero E6 cells. The dilution at which 50% of the cells showed cytopathic effect was averaged across 5 mice and graphed as the geometric mean titer for each vaccination group described in the legend of Fig. 6. * denotes a *P* value of <0.5. LOD, limit of detection.

to MERS-CoV infection in humans, and the animals do not succumb to infection (58–60). Additionally, because of ethical considerations, lower costs, and easier handling, mouse models are preferable over nonhuman primate (NHP) models for initial testing of vaccine candidates (61). MERS-CoV does not normally replicate in mice (62) due to species-specific differences in the DPP4 receptor; however, a mouse model using an adenovirus vector expressing hDPP4 has been created (50). This model relies on recombinant adenoviruses to transiently express hDPP4 in the lungs of normal or immunocompromised mice, which is followed by infection with MERS-CoV 5 days later. When we used this model to test vaccination with inactivated RABV virions containing MERS-CoV S1, our results demonstrated that vaccination was highly effective: it induced a strong antibody response against RABV G as well as MERS-CoV. Vaccination with the recombinant rabies virus vaccine reduced the viral titer of MERS-CoV in the lungs of vaccinated animals below detection levels.

The impact of the cellular immune response on protection against MERS-CoV is less clear, but previous studies have shown that vaccination with DNA or recombinant MVA expressing severe acute respiratory syndrome coronavirus (SARS-CoV) S induces strong cellular responses (22, 25). However, only adaptive-transfer experiments with specific cellular populations will allow a final conclusion on the effect of cellular immune responses against MERS-CoV infection.

Currently, several different vaccines against MERS-CoV are in development, but none of them are available for use. As for all vaccines, major considerations for their use include cost, safety, and immunogenicity. Viral vectors have been shown to be highly effective, but there are safety concerns. For instance, although different adenoviruses expressing MERS-

TABLE 1 RT-PCR for genomic RNA and mRNA after challenge with MERS-CoV

Group/immunization	MERS-CoV challenge	UpE RNA level		mRNA level	
		Mean	Standard deviation	Mean	Standard deviation
1/FILORAB1	Yes	17,871.24	12,935.90	506.73	353.30
2/BNSP333-S1	Yes	46.03	41.91	3.57	2.88
3/BNSP333-S1	No	23.52	25.97	1.83	2.17
4/PBS	Yes	12,047.57	3,833.46	357.89	116.37

TABLE 2 MERS-CoV recovered from lungs of immunized mice

Group/immunization	MERS-CoV challenge	Titer of recovered MERS-CoV[a]	
		Mean	Standard deviation
1/FILORAB1	Yes	7.65×10^6	4.04×10^2
2/BNSP333-S1	Yes	ND	
3/BNSP333-S1	No	ND	
4/PBS	Yes	7.65×10^6	2.09×10^2

[a]ND, not detected (the assay detection limit is 2.5×10^2 PFU/g of lung).

CoV S or S1 have been found to be immunogenic in mice, concerns include preexisting immunity and the longevity of the induced immune responses (30, 31). Preexisting immunity is not a major concern for MVA-based vectors, which are replication deficient in humans, but they may not be effective without multiple inoculations (22). DNA vaccines or recombinant MERS-CoV S protein-based vaccines are safest for immunocompromised individuals. DNA vaccines require relatively large amounts of DNA (e.g., 0.5 to 2 mg) and multiple inoculations in order to induce potent immune responses in mice and rhesus macaques (25). Other approaches with a recombinant S protein or subunits thereof have also been successfully studied as MERS-CoV vaccines. Finally, DNA vaccination followed by boosting with a recombinant protein is protective against MERS-CoV infection in rhesus macaques (16). Whereas all of these approaches have shown encouraging results, it remains to be seen whether they translate to a human MERS-CoV vaccine.

How does the current RABV-based MERS vaccine compare to other MERS-CoV vaccine approaches? Live RABV-based vaccines will probably not be considered for human use. Their proven efficacy in wildlife immunizations and their excellent safety record in different animal species do, however, make them good candidate animal vaccines. We are currently pursuing this approach using a dual vaccine against RABV and EBOV for apes, with encouraging results so far (P. D. Walsh, personal communication) (33). Based on our study, the inactivated rabies virus vaccine incorporating MERS-CoV S1 has efficacy in the adenovirus-DPP4 mouse model of MERS-CoV infection and appears to be promising for further MERS-CoV vaccine studies. The RABV vector itself has an excellent safety record, and more than 20 million individuals have been immunized against RABV. A similar inactivated vaccine is currently advancing to a phase 1 study for Ebola virus disease, FILORAB1, so additional safety data will become available in the near future.

MATERIALS AND METHODS

Cells and antibodies. Vero (ATCC CCL-81), Vero E6 (ATCC CRL-1586), and BSR (baby hamster kidney clone) cells were grown in Dulbecco modified Eagle medium (DMEM) supplemented with 5% (vol/vol) fetal bovine serum (FBS) and 1% (vol/vol) penicillin-streptomycin. Large virus stocks were prepared in Vero cells grown in serum-free Optipro medium (Invitrogen) supplemented with 20 mM glutamine and 1% (vol/vol) penicillin-streptomycin. Monoclonal antibody against the MERS-CoV spike protein was purchased from Alpha Diagnostics. Rabbit polyclonal antiserum against MERS-CoV S was purchased from Sinobiologicals. Monoclonal antibodies against rabies virus G were provided by Scott Dessain (Lankenau Medical Research Institute [LIMR], Wynnewood, PA). Monoclonal antibody against RABV phosphoprotein was a kind gift of Daniel Blondel (CNRS, Gif-Y-Survette, France).

cDNA construction of vaccine vectors. The vaccine vector BNSP333 was described previously (42). Full-length MERS-CoV spike protein cDNA and fragments of S with C-terminal truncations were amplified from a wild-type MERS-CoV cDNA clone provided by the Armed Forces Health Surveillance Center Division of Global Emerging Infections Surveillance and Response System. Primers were designed to include a BsiWI site at the 5′ end and an SpeI site at the 3′ end to allow insertion into BNSP333. The S1-RABV G chimera was assembled from codon-optimized cDNA encoding amino acids 1 to 750 of MERS-CoV S (Sinobiologicals) and codon-optimized cDNA encoding amino acids 428 to 524 of the RABV SAD-B19 glycoprotein (GenScript) by using overlap extension PCR. Recombinant clones were verified by DNA sequencing and used to recover infectious virus as described previously (45). Codons 18 to 750 of the spike protein gene were amplified by using codon-optimized cDNA as the template to generate the expression plasmid for the production of soluble S1. The PCR product was digested with BglII and NotI and cloned into the pDISPLAY vector (Invitrogen, Inc.).

Virus purification and inactivation. Recombinant RABVs were recovered as described previously (63). For large-scale purification of virus particles, 2-stack cell culture chambers were seeded with Vero cells (ATCC CCL-81) in DMEM supplemented with 5% fetal calf serum (FCS). Prior to the addition of virus, the cells were washed with PBS (Corning, Manassas, VA) and then infected at a low multiplicity of

infection (0.01 to 0.05) in serum-free medium at 34°C. The supernatant was collected at 3- to 4-day intervals and replaced with fresh serum-free medium. Cell culture media were centrifuged at low speed for 10 min to remove debris and filtered through 0.45-μm polyethersulfone (PES) membrane filters (Nalgene). The filtered supernatant was then concentrated by tangential-flow filtration in modified polyethersulfone (mPES) hollow-fiber cartridges (SpectrumLabs), followed by ultracentrifugation on 20% sucrose cushions in an SW32Ti rotor (Beckman) for 2 h at 25,000 rpm (106,000 $\times$ *g*). Pelleted virus was resuspended in PBS, and the protein content was measured by using a bicinchoninic acid (BCA) protein assay kit (Pierce) according to the manufacturer's instructions. Following the addition of PBS to adjust the protein concentration to 1 mg/ml, beta-propiolactone (BPL) was added at a concentration of 0.05% (vol/vol) to inactivate the virus. After overnight incubation at 4°C, inactivated particles were incubated at 37°C for 30 min and subsequently frozen in aliquots at −80°C. To verify the complete inactivation/absence of infectious virus, 10 μg of inactivated virus was inoculated into a flask seeded with BSR cells (baby hamster kidney cell clone). Four days after inoculation, 1/10 of the supernatant was passaged on fresh BSR cells. At 4 days postinoculation, the cells were fixed and stained with fluorescein isothiocyanate (FITC)-labeled monoclonal antibody against RABV nucleoprotein (Fujirebio).

One-step growth curves. Vero cell monolayers in T25 flasks were infected at an MOI of 5 for 1 h in Opti-MEM (Invitrogen, Carlsbad, CA). The inoculum was then removed, the monolayers were washed three times with serum-free medium to remove unadsorbed virus, and the medium was replaced with 5 ml DMEM containing 1% FCS. Samples of 200 μl were harvested from cell supernatants at the times indicated, and titers were determined in triplicate on Vero cells.

Protein gel analysis and Western blotting. Purified virus particles were denatured in urea buffer (125 mM Tris-HCl [pH 6.8], 8 M urea, 4% SDS, 5% beta-mercaptoethanol, 0.02% bromophenol blue) at 95°C for 5 min. Three micrograms of protein was then resolved on a 10% SDS-polyacrylamide gel and thereafter stained overnight with Sypro ruby (Lonza, Walkersville, MD) for total protein analysis or transferred onto a nitrocellulose membrane in Towbin buffer (192 mM glycine, 25 mM Tris, 20% methanol) for Western blot analysis. The nitrocellulose membrane was then blocked in Tris-buffered saline–Tween (TBST) (100 mM Tris-HCl [pH 7.9], 150 mM NaCl, 0.01% Tween 20) containing 5% (wt/vol) nonfat dried milk (AppliChem) at room temperature (RT) for 1 h. After blocking, the membrane was incubated overnight with a mixture of monoclonal antibodies 4C12, 4H3, and 8C5, specific for the RABV glycoprotein (kindly provided by Scott Dessain, Lankenau Medical Research Institute), or monoclonal antibody against the S1 subunit of MERS-CoV S (Alpha Diagnostics, Burlingame, CA) at a dilution of 1:1,000 in PBS containing 5% bovine serum albumin (BSA; Fisher Scientific). After washing, the blot was incubated for 1 h with the appropriate secondary antibody conjugated to horseradish peroxidase (HRP; Jackson ImmunoResearch) and diluted 1:20,000 in blocking buffer. Bands were developed with the SuperSignal West Dura chemiluminescent substrate (Pierce). Images were captured by using a FluorChem M charge-coupled-device (CCD) imaging system (ProteinSimple). A PageRuler prestained protein ladder (Thermo Scientific) was used for molecular weight determination.

Immunofluorescence. Vero E6 cells were seeded onto coverslips and infected the following day with MERS S-expressing RABV or control RABV in Opti-MEM at 34°C for 1 h. After the removal of the inoculum and the addition of fresh DMEM containing 5% FCS, the cells were incubated at 34°C for 48 h. At the end of the incubation, the cells were washed with PBS, fixed in 2% paraformaldehyde (PFA; Sigma) for 10 min, permeabilized in ice-cold methanol for 10 min at −20°C, washed with PBS, and blocked with PBS containing 5% BSA. The cells were then stained with mouse monoclonal antibody against MERS-CoV S1 (4 μg/ml in PBS containing 5% BSA) and Dylight488-conjugated monoclonal antibody 4C12 against the RABV glycoprotein for 1 to 2 h at RT. Following washing with PBS and incubation with Cy3-conjugated anti-mouse IgG secondary antibody (Jackson ImmunoResearch) (1:250 in PBS containing 5% BSA), the cells were mounted in Vectashield antifade solution (Vector Laboratories, Burlingame, CA). Images were acquired by using a Nikon C1 confocal microscope equipped with a 63$\times$ objective and a cooled CCD camera. Composite images were prepared by using ImageJ (64).

Sucrose density gradient analysis. BPL-inactivated particles were layered on top of a 16-ml linear 15 to 65% (wt/vol) sucrose gradient prepared by using a manual gradient maker (Jule, Inc., Milford, CT) in 16- by 102-mm centrifuge tubes. Brilliant Blue FCF was added to the 65% (wt/vol) sucrose solution to allow measurement of the sucrose concentration after fractionation. The gradient was centrifuged for 2 h at 106,000 $\times$ *g* in an SW32 rotor (Beckman), and 0.5-ml fractions were collected from the bottom of the tube. To precipitate proteins, 350 μl of each fraction was diluted with 1 ml water and mixed with 100 μl 100% (wt/vol) trichloroacetic acid. After incubation on ice for 1 h, the tubes were spun at 16,000 $\times$ *g* for 5 min. The supernatant was aspirated, and the pellets washed with acetone and resuspended in protein sample buffer (62.5 mM Tris-HCl [pH 6.8], 6 M urea, 2% [wt/vol] SDS, 5% [vol/vol] beta-mercaptoethanol, 0.01% [wt/vol] bromophenol blue) after brief drying at RT. Solubilized proteins were resolved by SDS-PAGE and subjected to Western blot analysis as described above by using rabbit polyclonal antiserum against RABV N and monoclonal antibodies against RABV G, RABV P, and MERS-CoV S1.

Electron microscopy. For sample evaluation by immunogold labeling, Vero E6 cells infected with RABV-MERS S1 were fixed *in situ* for 10 min (1.0% paraformaldehyde in Millonig's buffer; Tousimis Research, Rockville, MD). Fixed cells were incubated with rabbit polyclonal antiserum specific for MERS-CoV spike protein (Sinobiologicals) for 3 h at RT. The cells were washed with Cellgro Complete medium (Mediatech, Inc., Manassas, VA), incubated with goat anti-rabbit 15-nm colloidal gold (EM Sciences, Hatfield, PA) for 2 h at RT, washed, and incubated with human 4C12 anti-rabies virus primary antibody for 3 h at RT. Cells were washed again, incubated with goat anti-human 5-nm colloidal gold (EM Sciences) for 2 h at RT, washed, fixed for 2 h in 2.5% glutaraldehyde in Millonig's sodium phosphate buffer (Tousimis Research), scraped, and pelleted. Following fixation and staining, cells were washed by using Millonig's buffer, incubated for 2 h in 1.0%

osmium tetroxide, rinsed with ultrapure water, and *en bloc* stained with 2.0% uranyl acetate, and the samples were dehydrated in a series of graded ethanols, infiltrated, and embedded in DER-736 plastic resin. Embedded blocks were sectioned by using a Reichert-Jung Ultracut E ultramicrotome. Sections of 50 to 70 nm were collected on 200-mesh copper grids and poststained with Reynolds' lead citrate. Electron microscopy (EM) specimens were examined in an FEI Tecnai Spirit Twin transmission electron microscope operating at 80 kV.

Animal ethics statement. This study was carried out in strict accordance with recommendations described in the *Guide for the Care and Use of Laboratory Animals* (65) and by the Office of Animal Welfare and the U.S. Department of Agriculture. All animal work was approved by the Institutional Animal Care and Use Committees (IACUCs) at Thomas Jefferson University and at the University of Maryland School of Medicine. Mice were housed in cages in groups of five, under controlled humidity, temperature, and light (12-h light/12-h dark cycles) conditions. Food and water were available *ad libitum*.

Immunizations. Six- to eight-week-old female BALB/c mice were purchased from the Jackson Laboratory. Ten mice were inoculated intramuscularly with 10 μg of chemically inactivated BNSP333-S1-G particles in 100 μl PBS and boosted twice with the same amount of virus on day 7 and day 21, respectively. Groups of five mice were immunized with BNSP333-GP, BNSP333, or PBS as controls according to the same immunization schedule. Blood samples were collected by retro-orbital bleed immediately prior to the first immunization and at weekly intervals thereafter until day 35 postimmunization.

ELISA. Humoral responses to the RABV G and EBOV GP proteins were measured by an indirect ELISA as described previously (33). To determine antibody responses to the S protein of MERS-CoV, an indirect ELISA was developed by utilizing the purified S1 protein. The soluble S1 protein was produced by transfecting HEK293T cells with a plasmid that expresses a secreted S1 ectodomain (aa 18 to 750) fused to an N-terminal hemagglutinin (HA) tag. Purification of the HA-tagged protein from the supernatant of transfected cells was carried out as described previously (45). MaxiSorp 4 HBX 96-well plates (Nunc) were coated with 100 μl of purified S1 (0.5 μg/ml) in 50 mM carbonate buffer (pH 9.6) at 4°C overnight. Following washing with PBS containing 0.05% (wt/vol) Tween 20 (PBST) and blocking with PBST containing 5% dried milk, the plates were incubated overnight with 3-fold serial dilutions of mouse sera in PBS containing 0.5% (wt/vol) BSA. This was followed by three wash cycles, incubation with HRP-conjugated goat anti-mouse IgG secondary antibody (Jackson ImmunoResearch) (1:10,000 in PBST) for 2 h at RT, three more wash cycles, and the addition of the OPD (*o*-phenylenediamine dihydrochloride) substrate (Sigma-Aldrich). Color development was stopped by the addition of 50 μl of 3 M H_2SO_4 per well, and the optical density was measured at 490 nm by using an ELX800 plate reader (BioTek). Data were analyzed with GraphPad Prism (version 6.0), using 4-parameter nonlinear regression.

Infection and analysis of MERS-CoV replication in vaccinated mice. Vaccinated mice were transduced with an adenovirus vector by intranasal inoculation and left for 4 days to ensure the expression of DPP4, as described previously (50). Transduced mice were then infected with MERS-CoV (Jordan) as described previously (66), except that mice were inoculated with 2.5×10^3 PFU of MERS-CoV (Jordan) in a 50-μl total volume. At 4 days postinfection, MERS-CoV (Jordan) titers were determined by a plaque assay as described previously (66). MERS-CoV RNA levels were determined by PCR as described previously (66), except that the endogenous control was mouse transferrin receptor protein 1 (TFRC), using forward primer ATGACGTTGAA TTGAACCTGGACTA, reverse primer GTCTCCACGAGCGGAATACAG, and probe ABY-ATCAGGGATATGGGTCTA AGTCTACAGTGG-QSY in triplex with the previously described MERS-CoV primer/probe sets for the membrane (M) protein mRNA and an area upstream of the E gene (UpE) (67).

MERS-CoV neutralization assays. Sera from vaccinated mice were assessed for MERS-CoV neutralization activity as described previously (26).

Accession number(s). The GenBank accession numbers for BNSP333-S and BNSP333-S1 are KU696640 and KU696644, respectively.

ACKNOWLEDGMENTS

This work was supported in part by the U.S. National Institute of Allergy and Infectious Diseases (NIAID) Division of Intramural Research, the NIAID Division of Clinical Research, NIAID grant R01AI105204 to M.J.S., NIAID grant R01AI 5R01AI095569 to M.B.F., and the Jefferson Vaccine Center. This work was funded in part through Battelle Memorial Institute's prime contract with the NIAID under contract no. HHSN272200700016I. A subcontractor to Battelle Memorial Institute who performed this work is J.G.B., an employee of Tunnell Government Services, Inc. This work utilized the Bioimaging Shared Resource of the Sidney Kimmel Cancer Center (NCI 5 P30 CA-56036).

We thank Jennifer Wilson (Thomas Jefferson University, Philadelphia, PA) for critical reading and editing of the manuscript.

REFERENCES

1. Milne-Price S, Miazgowicz KL, Munster VJ. 2014. The emergence of the Middle East respiratory syndrome coronavirus. Pathog Dis 71:121–136. https://doi.org/10.1111/2049-632X.12166.
2. Zaki AM, van Boheemen S, Bestebroer TM, Osterhaus AD, Fouchier RA. 2012. Isolation of a novel coronavirus from a man with pneumonia in Saudi Arabia. N Engl J Med 367:1814–1820. https://doi.org/10.1056/NEJMoa1211721.
3. Anonymous. 2013. WHO statement on the third meeting of the IHR Emergency Committee concerning Middle East respiratory syndrome coronavirus (MERS-CoV). Wkly Epidemiol Rec 88:435–436.

4. Memish ZA, Zumla AI, Assiri A. 2013. Middle East respiratory syndrome coronavirus infections in health care workers. N Engl J Med 369:884–886. https://doi.org/10.1056/NEJMc1308698.
5. Drosten C, Kellam P, Memish ZA. 2014. Evidence for camel-to-human transmission of MERS coronavirus. N Engl J Med 371:1359–1360. https://doi.org/10.1056/NEJMc1409847.
6. Madani TA, Azhar EI, Hashem AM. 2014. Evidence for camel-to-human transmission of MERS coronavirus. N Engl J Med 371:1360. https://doi.org/10.1056/NEJMc1409847.
7. Azhar EI, El-Kafrawy SA, Farraj SA, Hassan AM, Al-Saeed MS, Hashem AM, Madani TA. 2014. Evidence for camel-to-human transmission of MERS coronavirus. N Engl J Med 370:2499–2505. https://doi.org/10.1056/NEJMoa1401505.
8. Khan A, Farooqui A, Guan Y, Kelvin DJ. 2015. Lessons to learn from MERS-CoV outbreak in South Korea. J Infect Dev Ctries 9:543–546. https://doi.org/10.3855/jidc.7278.
9. Park HY, Lee EJ, Ryu YW, Kim Y, Kim H, Lee H, Yi SJ. 2015. Epidemiological investigation of MERS-CoV spread in a single hospital in South Korea, May to June 2015. Euro Surveill 20(25):pii=21169. http://www.eurosurveillance.org/ViewArticle.aspx?ArticleId=21169.
10. Petersen E, Pollack MM, Madoff LC. 2014. Health-care associate transmission of Middle East respiratory syndrome corona virus, MERS-CoV, in the Kingdom of Saudi Arabia. Int J Infect Dis 29:299–300. https://doi.org/10.1016/j.ijid.2014.10.001.
11. Cauchemez S, Van Kerkhove MD, Riley S, Donnelly CA, Fraser C, Ferguson NM. 2013. Transmission scenarios for Middle East respiratory syndrome coronavirus (MERS-CoV) and how to tell them apart. Euro Surveill 18(24):pii=20503. http://www.eurosurveillance.org/ViewArticle.aspx?ArticleId=20503.
12. Ng DL, Al Hosani F, Keating MK, Gerber SI, Jones TL, Metcalfe MG, Tong S, Tao Y, Alami NN, Haynes LM, Mutei MA, Abdel-Wareth L, Uyeki TM, Swerdlow DL, Barakat M, Zaki SR. 2016. Clinicopathologic, immunohistochemical, and ultrastructural findings of a fatal case of Middle East respiratory syndrome coronavirus infection in the United Arab Emirates, April 2014. Am J Pathol 186:652–658. https://doi.org/10.1016/j.ajpath.2015.10.024.
13. Fett C, DeDiego ML, Regla-Nava JA, Enjuanes L, Perlman S. 2013. Complete protection against severe acute respiratory syndrome coronavirus-mediated lethal respiratory disease in aged mice by immunization with a mouse-adapted virus lacking E protein. J Virol 87:6551–6559. https://doi.org/10.1128/JVI.00087-13.
14. Almazan F, DeDiego ML, Sola I, Zuniga S, Nieto-Torres JL, Marquez-Jurado S, Andres G, Enjuanes L. 2013. Engineering a replication-competent, propagation-defective Middle East respiratory syndrome coronavirus as a vaccine candidate. mBio 4:e00650-13. https://doi.org/10.1128/mBio.00650-13.
15. Jimenez-Guardeno JM, Regla-Nava JA, Nieto-Torres JL, DeDiego ML, Castano-Rodriguez C, Fernandez-Delgado R, Perlman S, Enjuanes L. 2015. Identification of the mechanisms causing reversion to virulence in an attenuated SARS-CoV for the design of a genetically stable vaccine. PLoS Pathog 11:e1005215. https://doi.org/10.1371/journal.ppat.1005215.
16. Wang L, Shi W, Joyce MG, Modjarrad K, Zhang Y, Leung K, Lees CR, Zhou T, Yassine HM, Kanekiyo M, Yang ZY, Chen X, Becker MM, Freeman M, Vogel L, Johnson JC, Olinger G, Todd JP, Bagci U, Solomon J, Mollura DJ, Hensley L, Jahrling P, Denison MR, Rao SS, Subbarao K, Kwong PD, Mascola JR, Kong WP, Graham BS. 2015. Evaluation of candidate vaccine approaches for MERS-CoV. Nat Commun 6:7712. https://doi.org/10.1038/ncomms8712.
17. Modjarrad K. 2016. MERS-CoV vaccine candidates in development: the current landscape. Vaccine 34:2982–2987. https://doi.org/10.1016/j.vaccine.2016.03.104.
18. Du L, Jiang S. 2015. Middle East respiratory syndrome: current status and future prospects for vaccine development. Expert Opin Biol Ther 15:1647–1651. https://doi.org/10.1517/14712598.2015.1092518.
19. Enjuanes L, Zuniga S, Castano-Rodriguez C, Gutierrez-Alvarez J, Canton J, Sola I. 2016. Molecular basis of coronavirus virulence and vaccine development. Adv Virus Res 96:245–286. https://doi.org/10.1016/bs.aivir.2016.08.003.
20. Raj VS, Mou H, Smits SL, Dekkers DH, Muller MA, Dijkman R, Muth D, Demmers JA, Zaki A, Fouchier RA, Thiel V, Drosten C, Rottier PJ, Osterhaus AD, Bosch BJ, Haagmans BL. 2013. Dipeptidyl peptidase 4 is a functional receptor for the emerging human coronavirus-EMC. Nature 495:251–254. https://doi.org/10.1038/nature12005.
21. Burkard C, Verheije MH, Wicht O, van Kasteren SI, van Kuppeveld FJ, Haagmans BL, Pelkmans L, Rottier PJ, Bosch BJ, de Haan CA. 2014. Coronavirus cell entry occurs through the endo-/lysosomal pathway in a proteolysis-dependent manner. PLoS Pathog 10:e1004502. https://doi.org/10.1371/journal.ppat.1004502.
22. Volz A, Kupke A, Song F, Jany S, Fux R, Shams-Eldin H, Schmidt J, Becker C, Eickmann M, Becker S, Sutter G. 2015. Protective efficacy of recombinant modified vaccinia virus Ankara delivering Middle East respiratory syndrome coronavirus spike glycoprotein. J Virol 89:8651–8656. https://doi.org/10.1128/JVI.00614-15.
23. Ma C, Wang L, Tao X, Zhang N, Yang Y, Tseng CT, Li F, Zhou Y, Jiang S, Du L. 2014. Searching for an ideal vaccine candidate among different MERS coronavirus receptor-binding fragments—the importance of immunofocusing in subunit vaccine design. Vaccine 32:6170–6176. https://doi.org/10.1016/j.vaccine.2014.08.086.
24. Ma C, Li Y, Wang L, Zhao G, Tao X, Tseng CT, Zhou Y, Du L, Jiang S. 2014. Intranasal vaccination with recombinant receptor-binding domain of MERS-CoV spike protein induces much stronger local mucosal immune responses than subcutaneous immunization: implication for designing novel mucosal MERS vaccines. Vaccine 32:2100–2108. https://doi.org/10.1016/j.vaccine.2014.02.004.
25. Muthumani K, Falzarano D, Reuschel EL, Tingey C, Flingai S, Villarreal DO, Wise M, Patel A, Izmirly A, Aljuaid A, Seliga AM, Soule G, Morrow M, Kraynyak KA, Khan AS, Scott DP, Feldmann F, LaCasse R, Meade-White K, Okumura A, Ugen KE, Sardesai NY, Kim JJ, Kobinger G, Feldmann H, Weiner DB. 2015. A synthetic consensus anti-spike protein DNA vaccine induces protective immunity against Middle East respiratory syndrome coronavirus in nonhuman primates. Sci Transl Med 7:301ra132. https://doi.org/10.1126/scitranslmed.aac7462.
26. Coleman CM, Liu YV, Mu H, Taylor JK, Massare M, Flyer DC, Glenn GM, Smith GE, Frieman MB. 2014. Purified coronavirus spike protein nanoparticles induce coronavirus neutralizing antibodies in mice. Vaccine 32:3169–3174. https://doi.org/10.1016/j.vaccine.2014.04.016.
27. Du L, Zhao G, Kou Z, Ma C, Sun S, Poon VK, Lu L, Wang L, Debnath AK, Zheng BJ, Zhou Y, Jiang S. 2013. Identification of a receptor-binding domain in the S protein of the novel human coronavirus Middle East respiratory syndrome coronavirus as an essential target for vaccine development. J Virol 87:9939–9942. https://doi.org/10.1128/JVI.01048-13.
28. Yang Y, Deng Y, Wen B, Wang H, Meng X, Lan J, Gao GF, Tan W. 2014. The amino acids 736-761 of the MERS-CoV spike protein induce neutralizing antibodies: implications for the development of vaccines and antiviral agents. Viral Immunol 27:543–550. https://doi.org/10.1089/vim.2014.0080.
29. Zhang N, Channappanavar R, Ma C, Wang L, Tang J, Garron T, Tao X, Tasneem S, Lu L, Tseng CT, Zhou Y, Perlman S, Jiang S, Du L. 2016. Identification of an ideal adjuvant for receptor-binding domain-based subunit vaccines against Middle East respiratory syndrome coronavirus. Cell Mol Immunol 13:180–190. https://doi.org/10.1038/cmi.2015.03.
30. Kim E, Okada K, Kenniston T, Raj VS, AlHajri MM, Farag EA, AlHajri F, Osterhaus AD, Haagmans BL, Gambotto A. 2014. Immunogenicity of an adenoviral-based Middle East respiratory syndrome coronavirus vaccine in BALB/c mice. Vaccine 32:5975–5982. https://doi.org/10.1016/j.vaccine.2014.08.058.
31. Guo X, Deng Y, Chen H, Lan J, Wang W, Zou X, Hung T, Lu Z, Tan W. 2015. Systemic and mucosal immunity in mice elicited by a single immunization with human adenovirus type 5 or 41 vector-based vaccines carrying the spike protein of Middle East respiratory syndrome coronavirus. Immunology 145:476–484. https://doi.org/10.1111/imm.12462.
32. Pfaller CK, Cattaneo R, Schnell MJ. 2015. Reverse genetics of Mononegavirales: how they work, new vaccines, and new cancer therapeutics. Virology 479–480:331–344. https://doi.org/10.1016/j.virol.2015.01.029.
33. Willet M, Kurup D, Papaneri A, Wirblich C, Hooper JW, Kwilas SA, Keshwara R, Hudacek A, Beilfuss S, Rudolph G, Pommerening E, Vos A, Neubert A, Jahrling P, Blaney JE, Johnson RF, Schnell MJ. 2015. Preclinical development of inactivated rabies virus-based polyvalent vaccine against rabies and filoviruses. J Infect Dis 212(Suppl 2):S414–S424. https://doi.org/10.1093/infdis/jiv251.
34. Huttner A, Dayer JA, Yerly S, Combescure C, Auderset F, Desmeules J, Eickmann M, Finckh A, Goncalves AR, Hooper JW, Kaya G, Krahling V, Kwilas S, Lemaitre B, Matthey A, Silvera P, Becker S, Fast PE, Moorthy V, Kieny MP, Kaiser L, Siegrist CA, VSV-Ebola Consortium. 2015. The effect of dose on the safety and immunogenicity of the VSV Ebola candidate vaccine: a randomised double-blind, placebo-controlled phase 1/2 trial.

Lancet Infect Dis 15:1156–1166. https://doi.org/10.1016/S1473-3099(15)00154-1.
35. WHO. 2015. Rabies, fact sheet #99. WHO, Geneva, Switzerland.
36. Cliquet F, Aubert M. 2004. Elimination of terrestrial rabies in Western European countries. Dev Biol (Basel) 119:185–204.
37. Blaney JE, Marzi A, Willet M, Papaneri AB, Wirblich C, Feldmann F, Holbrook M, Jahrling P, Feldmann H, Schnell MJ. 2013. Antibody quality and protection from lethal Ebola virus challenge in nonhuman primates immunized with rabies virus based bivalent vaccine. PLoS Pathog 9:e1003389. https://doi.org/10.1371/journal.ppat.1003389.
38. Blaney JE, Wirblich C, Papaneri AB, Johnson RF, Myers CJ, Juelich TL, Holbrook MR, Freiberg AN, Bernbaum JG, Jahrling PB, Paragas J, Schnell MJ. 2011. Inactivated or live-attenuated bivalent vaccines that confer protection against rabies and Ebola viruses. J Virol 85:10605–10616. https://doi.org/10.1128/JVI.00558-11.
39. Papaneri AB, Wirblich C, Cann JA, Cooper K, Jahrling PB, Schnell MJ, Blaney JE. 2012. A replication-deficient rabies virus vaccine expressing Ebola virus glycoprotein is highly attenuated for neurovirulence. Virology 434:18–26. https://doi.org/10.1016/j.virol.2012.07.020.
40. Papaneri AB, Wirblich C, Cooper K, Jahrling PB, Schnell MJ, Blaney JE. 2012. Further characterization of the immune response in mice to inactivated and live rabies vaccines expressing Ebola virus glycoprotein. Vaccine 30:6136–6141. https://doi.org/10.1016/j.vaccine.2012.07.073.
41. Conzelmann KK, Cox JH, Schneider LG, Thiel HJ. 1990. Molecular cloning and complete nucleotide sequence of the attenuated rabies virus SAD B19. Virology 175:485–499. https://doi.org/10.1016/0042-6822(90)90433-R.
42. McGettigan JP, Pomerantz RJ, Siler CA, McKenna PM, Foley HD, Dietzschold B, Schnell MJ. 2003. Second-generation rabies virus-based vaccine vectors expressing human immunodeficiency virus type 1 Gag have greatly reduced pathogenicity but are highly immunogenic. J Virol 77:237–244. https://doi.org/10.1128/JVI.77.1.237-244.2003.
43. Hudacek AW, Al-Saleem FH, Willet M, Eisemann T, Mattis JA, Simpson LL, Schnell MJ. 2014. Recombinant rabies virus particles presenting botulinum neurotoxin antigens elicit a protective humoral response in vivo. Mol Ther Methods Clin Dev 1:14046. https://doi.org/10.1038/mtm.2014.46.
44. McGettigan JP, Naper K, Orenstein J, Koser M, McKenna PM, Schnell MJ. 2003. Functional human immunodeficiency virus type 1 (HIV-1) Gag-Pol or HIV-1 Gag-Pol and Env expressed from a single rhabdovirus-based vaccine vector genome. J Virol 77:10889–10899. https://doi.org/10.1128/JVI.77.20.10889-10899.2003.
45. Kurup D, Wirblich C, Feldmann H, Marzi A, Schnell MJ. 2015. Rhabdovirus-based vaccine platforms against henipaviruses. J Virol 89:144–154. https://doi.org/10.1128/JVI.02308-14.
46. Qian Z, Dominguez SR, Holmes KV. 2013. Role of the spike glycoprotein of human Middle East respiratory syndrome coronavirus (MERS-CoV) in virus entry and syncytia formation. PLoS One 8:e76469. https://doi.org/10.1371/journal.pone.0076469.
47. Servat A, Feyssaguet M, Blanchard I, Morize JL, Schereffer JL, Boue F, Cliquet F. 2007. A quantitative indirect ELISA to monitor the effectiveness of rabies vaccination in domestic and wild carnivores. J Immunol Methods 318:1–10. https://doi.org/10.1016/j.jim.2006.07.026.
48. Wasniewski M, Cliquet F. 2012. Evaluation of ELISA for detection of rabies antibodies in domestic carnivores. J Virol Methods 179:166–175. https://doi.org/10.1016/j.jviromet.2011.10.019.
49. Wasniewski M, Guiot AL, Schereffer JL, Tribout L, Mahar K, Cliquet F. 2013. Evaluation of an ELISA to detect rabies antibodies in orally vaccinated foxes and raccoon dogs sampled in the field. J Virol Methods 187:264–270. https://doi.org/10.1016/j.jviromet.2012.11.022.
50. Zhao J, Li K, Wohlford-Lenane C, Agnihothram SS, Fett C, Gale MJ, Jr, Baric RS, Enjuanes L, Gallagher T, McCray PB, Jr, Perlman S. 2014. Rapid generation of a mouse model for Middle East respiratory syndrome. Proc Natl Acad Sci U S A 111:4970–4975. https://doi.org/10.1073/pnas.1323279111.
51. Smith ME, Koser M, Xiao S, Siler C, McGettigan JP, Calkins C, Pomerantz RJ, Dietzschold B, Schnell MJ. 2006. Rabies virus glycoprotein as a carrier for anthrax protective antigen. Virology 353:344–356. https://doi.org/10.1016/j.virol.2006.05.010.
52. McKenna PM, Pomerantz RJ, Dietzschold B, McGettigan JP, Schnell MJ. 2003. Covalently linked human immunodeficiency virus type 1 gp120/gp41 is stably anchored in rhabdovirus particles and exposes critical neutralizing epitopes. J Virol 77:12782–12794. https://doi.org/10.1128/JVI.77.23.12782-12794.2003.
53. Siler CA, McGettigan JP, Dietzschold B, Herrine SK, Dubuisson J, Pomerantz RJ, Schnell MJ. 2002. Live and killed rhabdovirus-based vectors as potential hepatitis C vaccines. Virology 292:24–34. https://doi.org/10.1006/viro.2001.1212.
54. Schnell MJ, Foley HD, Siler CA, McGettigan JP, Dietzschold B, Pomerantz RJ. 2000. Recombinant rabies virus as potential live-viral vaccines for HIV-1. Proc Natl Acad Sci U S A 97:3544–3549. https://doi.org/10.1073/pnas.97.7.3544.
55. Winter C, Schwegmann-Wessels C, Neumann U, Herrler G. 2008. The spike protein of infectious bronchitis virus is retained intracellularly by a tyrosine motif. J Virol 82:2765–2771. https://doi.org/10.1128/JVI.02064-07.
56. Schwegmann-Wessels C, Ren X, Herrler G. 2006. Intracellular transport of the S proteins of coronaviruses. Adv Exp Med Biol 581:271–275. https://doi.org/10.1007/978-0-387-33012-9_45.
57. Schwegmann-Wessels C, Al-Falah M, Escors D, Wang Z, Zimmer G, Deng H, Enjuanes L, Naim HY, Herrler G. 2004. A novel sorting signal for intracellular localization is present in the S protein of a porcine coronavirus but absent from severe acute respiratory syndrome-associated coronavirus. J Biol Chem 279:43661–43666. https://doi.org/10.1074/jbc.M407233200.
58. Munster VJ, de Wit E, Feldmann H. 2013. Pneumonia from human coronavirus in a macaque model. N Engl J Med 368:1560–1562. https://doi.org/10.1056/NEJMc1215691.
59. de Wit E, Rasmussen AL, Falzarano D, Bushmaker T, Feldmann F, Brining DL, Fischer ER, Martellaro C, Okumura A, Chang J, Scott D, Benecke AG, Katze MG, Feldmann H, Munster VJ. 2013. Middle East respiratory syndrome coronavirus (MERS-CoV) causes transient lower respiratory tract infection in rhesus macaques. Proc Natl Acad Sci U S A 110:16598–16603. https://doi.org/10.1073/pnas.1310744110.
60. Falzarano D, de Wit E, Rasmussen AL, Feldmann F, Okumura A, Scott DP, Brining D, Bushmaker T, Martellaro C, Baseler L, Benecke AG, Katze MG, Munster VJ, Feldmann H. 2013. Treatment with interferon-alpha2b and ribavirin improves outcome in MERS-CoV-infected rhesus macaques. Nat Med 19:1313–1317. https://doi.org/10.1038/nm.3362.
61. Baseler L, de Wit E, Feldmann H. 2016. A comparative review of animal models of Middle East respiratory syndrome coronavirus infection. Vet Pathol 53:521–531. https://doi.org/10.1177/0300985815620845.
62. Coleman CM, Matthews KL, Goicochea L, Frieman MB. 2014. Wild-type and innate immune-deficient mice are not susceptible to the Middle East respiratory syndrome coronavirus. J Gen Virol 95:408–412. https://doi.org/10.1099/vir.0.060640-0.
63. Papaneri AB, Wirblich C, Marissen WE, Schnell MJ. 2013. Alanine scanning of the rabies virus glycoprotein antigenic site III using recombinant rabies virus: implication for post-exposure treatment. Vaccine 31:5897–5902. https://doi.org/10.1016/j.vaccine.2013.09.038.
64. Schneider CA, Rasband WS, Eliceiri KW. 2012. NIH Image to ImageJ: 25 years of image analysis. Nat Methods 9:671–675. https://doi.org/10.1038/nmeth.2089.
65. National Research Council. 2011. Guide for the care and use of laboratory animals, 8th ed. National Academies Press, Washington, DC.
66. Pascal KE, Coleman CM, Mujica AO, Kamat V, Badithe A, Fairhurst J, Hunt C, Strein J, Berrebi A, Sisk JM, Matthews KL, Babb R, Chen G, Lai KM, Huang TT, Olson W, Yancopoulos GD, Stahl N, Frieman MB, Kyratsous CA. 2015. Pre- and postexposure efficacy of fully human antibodies against spike protein in a novel humanized mouse model of MERS-CoV infection. Proc Natl Acad Sci U S A 112:8738–8743. https://doi.org/10.1073/pnas.1510830112.
67. Coleman CM, Frieman MB. 2015. Growth and quantification of MERS-CoV infection. Curr Protoc Microbiol 37:15E.2.1–15E.2.9. https://doi.org/10.1002/9780471729259.mc15e02s37.